

# Triethylenetetramine penta- and hexa-acetamide ligands and their ytterbium complexes as paraCEST contrast agents for MRI†

Dirk Burdinski,<sup>\*a</sup> Johan Lub,<sup>a</sup> Jeroen A. Pikkemaat,<sup>b</sup> Diana Moreno Jalón,<sup>a</sup> Sophie Martial<sup>a</sup> and Carolina Del Pozo Ochoa<sup>a</sup>

Received 29th February 2008, Accepted 16th April 2008

First published as an Advance Article on the web 12th June 2008

DOI: 10.1039/b803557a

The ligand triethylenetetramine-*N,N,N',N'',N''',N''''*-hexaacetamide (ttham) was synthesized with the aim of forming lanthanide complexes suitable as contrast agents for magnetic resonance imaging applications utilizing the chemical exchange-dependent saturation transfer (CEST) effect. It was designed to exclude water molecules from the first coordination sphere and provide a high number of CEST active amide protons per lanthanide ion. The ligand was characterized by its protonation behavior and its complexation properties with ytterbium ions in aqueous solution. The basicity of the ttham backbone amine protons decreases in the order  $N_{\text{central}(1)} > N_{\text{terminal}(1)} > N_{\text{terminal}(2)} > N_{\text{central}(2)}$ , as deduced from NMR titration experiments and from a comparison of its protonation constants with those of two ttham derivatives, in which either a terminal (*N*-benzyl-triethylenetetramine-*N,N',N'',N''',N''''*-pentaacetamide, 1btppam) or a central acetamide group (*N'*-benzyl-triethylenetetramine-*N,N',N'',N''',N''''*-pentaacetamide, 4btppam) is substituted with a benzyl group. This protonation sequence results from the combined influence of inductive effects, the intramolecular hydrogen bonding network, and the Coulomb repulsion between protonated ammonium groups. The ytterbium complex of ttham, [Yb(ttham)]Cl<sub>3</sub>, is coordinatively frustrated. Due to steric constraints, in addition to the four backbone nitrogen atoms, only three of the four symmetry-equivalent terminal acetamide donors can coordinate simultaneously to the ytterbium ion, and the dangling fourth one exchanges quickly with the other three. The ytterbium complexes of a total of five ligands (ttham, 1btppam, 4btppam, 2,2',2''-triaminotriethylaminehexaacetamide (ttaham), and diethylenetriamine-*N,N,N',N'',N''',N''''*-pentaacetamide (dtpam)) were studied with respect to their CEST properties. In solution, all of these complexes have a low symmetry. The presence of multiple magnetically different amide groups in each complex prevents the realization of very high CEST effects. These results nevertheless form an excellent basis for a further optimization of this class of ligands.

## Introduction

The majority of current magnetic resonance imaging (MRI) contrast agents (CAs) are based on paramagnetic gadolinium complexes. These complexes shorten the relaxation time of bulk water protons in tissue by utilizing water molecules that are weakly coordinated and exchange rapidly with those of the bulk water pool.<sup>1–3</sup> In recent years, a conceptually new class of MRI CAs that is based on chemical exchange-dependent saturation transfer (CEST) has attracted much attention.<sup>4–6</sup> In the presence of a CEST agent the signal intensity of the bulk water protons can be altered by selectively saturating, with a strong radio frequency (RF) pulse, the resonance frequency of mildly acidic protons of the CEST agent, which are in an intermediately fast exchange equilibrium with bulk water. The magnitude of the magnetization transfer, the CEST effect, is usually calculated according to eqn (1).<sup>5</sup>

$$\% \text{CEST} = (M_0 - M_S) / M_\infty \times 100\% \quad (1)$$

$M_S$  is the intensity of the magnetic resonance (MR) signal of the bulk water taken immediately after an RF saturation pulse has been applied at the resonance frequency of the CA's exchangeable protons.  $M_0$  is the intensity of the reference signal that is recorded after the RF saturation pulse has been applied symmetrically on the opposite side of the bulk water signal to correct for non-selective saturation, most prominently direct water saturation, and  $M_\infty$  is the intensity of a second reference MR signal that is recorded at a significantly different frequency that is not affected by magnetization transfer effects.

In a two-site exchange model, at complete saturation of the exchangeable proton resonance, and in the absence of direct saturation of the bulk water resonance and background magnetization transfer,  $M_S/M_\infty$  is given by eqn (2a) and eqn (2b).<sup>7,8</sup>

$$M_S/M_\infty = 1/(1 + k_{\text{ex}} T_{1\text{sat}}) \quad (2a)$$

$$k_{\text{ex}} = n[\text{CA}]/2[\text{H}_2\text{O}]\tau_M \quad (2b)$$

$T_{1\text{sat}}$  is the spin–lattice relaxation time of the bulk water protons during saturation of the exchanging protons and  $k_{\text{ex}}$  is the pseudo-first-order exchange rate constant, where  $[\text{H}_2\text{O}]$  is

<sup>a</sup>Department of Bio-Molecular Engineering, Philips Research, High Tech Campus, 5656 AE, Eindhoven, The Netherlands. E-mail: dirk.burdinski@philips.com

<sup>b</sup>Department of Materials Analysis, Philips Research, High Tech Campus, 5656 AE, Eindhoven, The Netherlands

† Electronic supplementary information (ESI) available: Fig. S1–S3. See DOI: 10.1039/b803557a

the concentration of the bulk water,  $[CA]$  is the concentration of the CEST CA,  $n$  is the number and  $\tau_M$  is the life time of the exchangeable protons. The coordination of suitable CEST-active structures to a paramagnetic lanthanide ion in so called paraCEST agents increases the sensitivity of low molecular weight CEST agents by allowing higher exchange rates ( $k_{ex}$ ) of the CEST-active protons with paramagnetically shifted resonance frequencies without exceeding the optimum proton exchange range ( $|k_{ex}| < |\omega(H_{ex}) - \omega(H_2O)|$ ).<sup>9,10</sup>

A general advantage of CEST-based CAs over paramagnetic relaxation agents is that the image contrast can be switched on and off at will, which is particularly interesting for molecular imaging applications. The information obtained with this specific contrast-enhancement technique can be immediately correlated with an unenhanced reference image, which can be measured without time delay. In this context, strategies have been devised to modulate the paraCEST effect in response to a physiologically meaningful parameter, such as pH,<sup>11–13</sup> temperature,<sup>14</sup> metabolite concentration,<sup>15</sup> or enzyme activity.<sup>16</sup>

A number of approaches have been described to increase the sensitivity of known paraCEST agents into the range that makes them attractive for molecular imaging applications. A very promising strategy is to increase the number  $n$  of CEST-active protons [eqn (2b)] per agent by utilizing polymeric or dendritic agents or by preparing nanoparticles that are decorated with a large number of small molecule paraCEST agents.<sup>13,17–19</sup> Poly(propylene imine) dendrimers, covalently functionalized with up to 16 CEST-active Yb complexes, were reported to show a decrease of the lowest detectable concentration that was proportional to the number of Yb complexes per molecule.<sup>13</sup> The therein employed Yb complex is derived from  $[Yb(\text{dotam})(H_2O)]^{3+}$  (Chart 1), the archetypal small molecule paraCEST agent.<sup>20,21</sup> Of the lanthanide ions, ytterbium allows for the highest practical CEST effect, in part due to its comparably small magnetic moment and the related long  $T_1$  values in aqueous solution.<sup>22</sup> The unsubstituted Yb-dotam

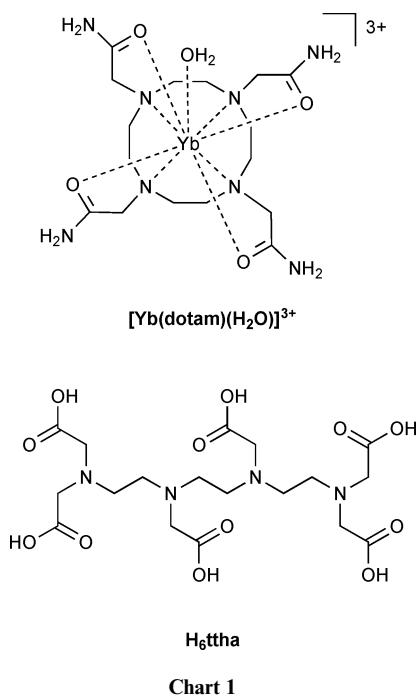
complex bears a total of eight CEST-active amide protons on the four equivalent acetamide pendent arms. Dotam and most of its numerous and intensively studied derivatives are octadentate ligands and allow for the further coordination of at least one aqua ligand to the encapsulated lanthanide ion, which is a rudiment of the need for an exchangeable water molecule in the gadolinium complex of the parent ligand 1,4,7,10-tetraazacyclododecane-1,4,7,10-tetra(acetic acid) ( $H_4\text{dota}$ ), a clinically used  $T_1$  CA (Dotarem<sup>TM</sup>, Guerbet). In contrast to conventional gadolinium-based  $T_1$  CAs, such amide-based paraCEST agents do not require a coordination site for water exchange. Its presence is even unfavorable, due to lanthanide-induced relaxation mediated by the weakly coordinated water molecule.<sup>22</sup> Such  $T_1$  relaxation reduces the magnetic saturation that is built up with the preparative RF pulse and thereby limits the achievable CEST effect [eqn (2a)].

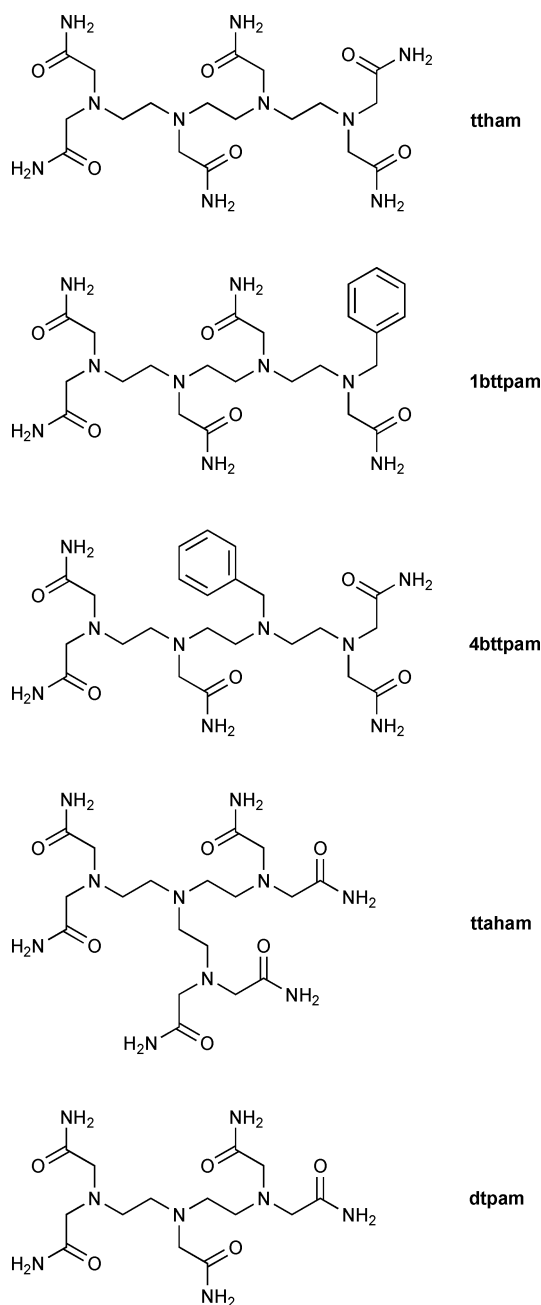
It was therefore an aim of this study to develop a new ligand system for paraCEST agents that would exclude water molecules from the first coordination sphere, at the same time increase the number  $n$  of CEST active amide protons per lanthanide ion [eqn (2b)], and allow for the introduction of linker groups for a straightforward coupling to targeting bio-active ligands. We considered the hexaamide derivative, ttham (Chart 2), of the known decadentate ligand triethylenetetramine- $N,N,N',N'',N''',N''''$ -hexa(acetic acid) ( $H_6\text{ttha}$ , Chart 1) to be a good candidate.<sup>23,24</sup> The  $H_6\text{ttha}$  ligand forms nonacoordinate complexes with the late lanthanide ions, in which it typically saturates the first coordination sphere by binding to the metal *via* the four backbone amino groups as well as the oxygen atoms of five of the six carboxylate groups.<sup>25–28</sup> A similar mode of coordination to ytterbium ions was therefore expected for the ttham ligand. In such an arrangement the sixth, dangling pendent arm would then be available for further chemical modification of the probe with little impact on the CEST properties of the core complex. To test this property, two ttham derivatives were synthesized, in each of which one of the two different acetamide groups was substituted with a non-coordinating benzyl group, rendering the ligand potentially nonadentate. The ytterbium complexes of ttham, of its two benzyl derivatives, and of two related new reference ligands (Chart 2) were synthesized and studied with respect to their NMR and CEST properties.

## Experimental

All solvents were obtained from Merck. 4-Morpholinepropanesulfonic acid (MOPS, 99.5%) and all other commercial chemicals were obtained from Sigma-Aldrich in the highest available quality. Di-*tert*-butyl 2-bromoethylamine- $N,N$ -diacetate (**12**),<sup>29</sup>  $K_3[Yb(\text{ttha})]$ ,<sup>25</sup> dotam,<sup>30</sup> and  $[Yb(\text{dotam})(H_2O)]Cl_3$ <sup>31</sup> were prepared following published procedures.

pD values in  $D_2O$  solutions were calculated ( $pD = pH^D + 0.4$ ) from operational pH values ( $pH^D$ ) measured with a WTW SenTix Mic glass electrode linked to a WTW pH 315i pH meter.<sup>32,33</sup> NMR spectra for structure verification were recorded using a Bruker DPX300 spectrometer of solutions in deuterated solvents (dichloromethane, chloroform, or dimethyl sulfoxide). FT-IR spectra were recorded on an ATI Mattson Genesis II spectrometer. Reported absorption bands were sharp and exhibited medium to strong intensity, unless noted otherwise (w = weak, br = broad). MALDI-TOF mass spectra were recorded on a Voyager-DE-Pro





(PerSeptive Biosystems, Perkin-Elmer) machine using  $\alpha$ -cyano-4-hydroxycinnamic acid as a matrix and a positive reflector mode detection method. ESI mass spectra were recorded on an LCQ Deca XP Max (Thermo Finnigan) machine using an  $\text{H}_2\text{O}-\text{CH}_3\text{CN}$  (1 : 1) mixture as the solvent and an injection rate of  $0.05 \text{ cm}^3 \text{ min}^{-1}$ .

### Elemental analysis

The chloride content was determined by ion chromatography of aqueous solutions against calibration standards. The yttrium content was determined by inductively coupled plasma-atomic emission spectroscopy (ICP-AES). In preparation for ICP-AES analysis, material samples were heated with hydrochloric acid at

$128 \text{ }^\circ\text{C}$  for 2 h. Then a small amount of 70% perchloric acid was added and the temperature was raised to  $180 \text{ }^\circ\text{C}$  for 1 d. The obtained solutions were cooled and diluted with water to a known volume. C, H, N analyses were performed by means of conductivity measurement after combustion of the material with a plug of oxygen and separation of the combustion gases.

### Potentiometry

Titration curves were carried out in a water jacket  $10 \text{ cm}^3$  titration vessel maintained at  $25.0 \pm 0.1 \text{ }^\circ\text{C}$ , using a 716 DMS Titrino automatic titrator (Metrohm), which was coupled to a PC controlled by the VESUV 3.0 titration software (Metrohm). The “Dynamic Equivalent point Titration” (DET) method was chosen optimized to achieve the maximum sensitivity for weak equivalent points. Titrations were carried out with  $0.1002 \text{ M HCl}$  in  $0.1 \text{ M NaNO}_3$  solution under Ar to exclude atmospheric  $\text{CO}_2$ . During titrations the pH was recorded with a Metrohm “LL combined pH glass electrode” (type 6.0233.100), which was calibrated with a series of 9 pH buffers (Merck), ranging from pH 1.00–9.00. The accuracy of the pH measurements was  $\pm 0.01 \text{ pH}$ . Equivalence points in the titration curve were evaluated based on the zero crossing of the second derivative (after correction for curve distortion) using the VESUV titration software package. The calculation of the  $\log K$  values by the software is based on the Henderson–Hasselbalch relation between activities of a conjugated acid–base pair in aqueous solution.

### CEST NMR spectroscopy

Samples were prepared by dissolving the appropriate amount of yttrium complex in  $20 \text{ mM MOPS}$  buffer (pH 7.40). If required, the pH values of the solutions were adjusted by adding small aliquots of either  $0.1 \text{ M NaOH}$  or  $0.1 \text{ M HCl}$  stock solutions. To enable frequency locking, a coaxial glass capillary insert filled with deuterated tetrachloroethane was used. NMR spectra were recorded on a Bruker Avance NMR spectrometer equipped with an Oxford wide-bore 7 T superconducting magnet.  $1\text{D } ^1\text{H}$  NMR measurements were performed without water suppression. Complex data points (128k) were acquired with a dwell time of  $200 \text{ } \mu\text{s}$ . Prior to Fourier transform, the data were apodized with an exponential filter (line broadening =  $5 \text{ Hz}$ ). All spectra were calibrated relative to the  $\text{H}_2\text{O}$  frequency. CEST spectra were recorded using standard continuous-wave irradiation ( $2 \text{ s}$  pulse duration;  $22.1 \text{ } \mu\text{T}$  pulse amplitude) for selective presaturation of the exchangeable-proton resonances. Of the Yb complexes of ttham, 1bttpam, and 4bttpam, 511 individual  $1\text{D } ^1\text{H}$  NMR spectra were acquired at different values of the presaturation offset frequency ( $500 \text{ Hz}$  intervals up to  $127.5 \text{ kHz}$ ) centered around the water resonance frequency and stored in a single  $2\text{D}$  NMR data set. Of the Yb complexes of dtpam and ttaham, 149 individual  $1\text{D } ^1\text{H}$  NMR spectra were acquired at different values of the presaturation offset frequency ( $200 \text{ Hz}$  intervals up to  $10 \text{ kHz}$ , then  $1000 \text{ Hz}$  intervals up to  $100 \text{ kHz}$ ). To reconstruct the CEST spectrum, the water signal of each individual spectrum in the  $2\text{D}$  data set was integrated and plotted as a function of the presaturation offset frequency. From the resulting spectrum the CEST effect was determined using eqn (1).

## Syntheses

**Hexaethyl triethylenetetramine-*N,N,N',N'',N''',N''''*-hexaacetate (2).** A mixture of triethylenetetramine-*N,N,N',N'',N''',N''''*-hexaacetic acid (**1**) (20.0 g, 40.4 mmol), concentrated sulfuric acid (9.0 cm<sup>3</sup>, 0.17 mol), and ethanol (400 cm<sup>3</sup>) was refluxed in a nitrogen atmosphere for 20 h. The reaction mixture was concentrated under reduced pressure at 45 °C and diluted with dichloromethane (150 cm<sup>3</sup>). The obtained solution was extracted with 1.5 N NaOH solution (250 cm<sup>3</sup>) and brine (100 cm<sup>3</sup>). Drying of the organic layer over magnesium sulfate, filtration over a short neutral alumina column, and evaporation of the solvent yielded **2** as a yellow oil (22.4 g, 84%). <sup>1</sup>H NMR (CDCl<sub>3</sub>, δ/ppm): 4.16 (q, *J* = 7.1 Hz, 8H), 4.14 (q, *J* = 7.1 Hz, 4H), 3.57 (s, 8H), 3.44 (s, 4H), 2.85 (t, *J* = 6.0 Hz, 4H), 2.78 (t, *J* = 6.0 Hz, 4H), 2.74 (s, 4H), 1.27 (t, *J* = 7.1 Hz, 12H), 1.26 (t, *J* = 7.1 Hz, 6H).

**Triethylenetetramine-*N,N,N',N'',N''',N''''*-hexaacetamide (ttham).** A solution of **2** (22.4 g, 33.8 mmol) in 7 N ammonia in methanol (300 cm<sup>3</sup>) was stirred at RT for 9 d. A precipitate was formed, which was collected by filtration, washed with methanol (200 cm<sup>3</sup>), and dried over silica. The product was obtained as a white powder (5.4 g, 33%). FT-IR (ATR, cm<sup>-1</sup>): 3387 (NH<sub>2</sub>), 1679 and 1635 (C=O). MS (MALDI-TOF, *m/z*): Calcd for C<sub>18</sub>H<sub>36</sub>N<sub>10</sub>O<sub>6</sub><sup>+</sup>: 488.28. Found: 488.19. <sup>1</sup>H NMR (DMSO-*d*<sub>6</sub>, δ/ppm): 7.60 (s, 4H), 7.28 (s, 2H), 7.10 (s, 4H), 7.03 (s, 2H), 3.03 (s, 8H), 2.96 (s, 4H), 2.56 (s, 8H), 2.54 (s, 4H). <sup>13</sup>C NMR (DMSO-*d*<sub>6</sub>, δ/ppm): 173.4, 173.2, 59.2, 58.4, 53.3, 53.2, 53.1.

**Pentaethyl diethylenetriamine-*N,N,N',N'',N'''*-pentaacetate (4).** This compound was obtained as a yellow oil in 76% yield following the synthesis protocol of **2**, using diethylenetriamine-*N,N,N',N'',N'''*-pentaacetic acid (**3**) instead of triethylenetetramine-*N,N,N',N'',N''',N''''*-hexaacetic acid (**1**). <sup>1</sup>H NMR (CDCl<sub>3</sub>, δ/ppm): 4.16 (q, *J* = 7.1 Hz, 8H), 4.14 (q, *J* = 7.1 Hz, 2H), 3.57 (s, 8H), 3.47 (s, 2H), 2.85 (t, *J* = 5.7 Hz, 4H), 2.79 (t, *J* = 5.7 Hz, 4H), 1.27 (t, *J* = 7.1 Hz, 12H), 1.26 (t, *J* = 7.1 Hz, 3H).

**Diethylenetriamine-*N,N,N',N'',N'''*-pentaacetamide (dtpam).** This compound was obtained as a white powder in 53% yield following the synthesis protocol of ttham, using **4** instead of **2**. FT-IR (ATR, cm<sup>-1</sup>): 3337 (NH<sub>2</sub>), 1658 (C=O). MS (MALDI-TOF, *m/z*): Calcd for C<sub>14</sub>H<sub>28</sub>N<sub>8</sub>O<sub>5</sub><sup>+</sup>: 388.22. Found: 388.15. <sup>1</sup>H NMR (DMSO-*d*<sub>6</sub>, δ/ppm): 7.60 (s, 4H), 7.28 (s, 1H), 7.10 (s, 4H), 7.04 (s, 1H), 3.05 (s, 8H), 2.93 (s, 2H), 2.56 (s, 8H). <sup>13</sup>C NMR (DMSO-*d*<sub>6</sub>, δ/ppm): 173.4, 173.2, 59.2, 58.4, 53.2, 53.1.

**Hexaethyl 2,2',2''-triaminotriethylaminehexaacetate (6).** 2,2',2''-Triaminotriethylamine (**5**) (3.08 g, 21.1 mmol) was added dropwise to a vigorously stirred mixture of ethyl bromoacetate (21.1 g, 126 mmol), potassium bicarbonate (24.8 g, 248 mmol), and DMF (90 cm<sup>3</sup>), which was cooled in an ice–water bath. Stirring was continued for 1 h in an ice–water bath and subsequently for 48 h at RT. Following evaporation of the DMF (60 °C, 7 mbar), toluene (90 cm<sup>3</sup>) and water (150 cm<sup>3</sup>) were added. After separation, the organic layer was extracted with water (2 × 100 cm<sup>3</sup>) and brine (100 cm<sup>3</sup>). Drying of the organic layer over magnesium sulfate and evaporation of the solvents afforded pure **6** as a yellow oil (9.15 g, 65%). <sup>1</sup>H NMR (CDCl<sub>3</sub>, δ/ppm): 4.14 (q, *J* = 7.1 Hz, 12H), 3.58

(s, 12H), 2.81 (t, *J* = 6.3 Hz, 6H), 2.62 (t, *J* = 6.3 Hz, 6H), 1.27 (t, *J* = 7.1 Hz, 18H).

**2,2',2''-Triaminotriethylaminehexaacetamide (ttaham).** A solution of **6** (1.82 g, 2.75 mmol) in 7 N ammonia in methanol (14 cm<sup>3</sup>) was stirred at RT for 9 d. Evaporation of the volatiles yielded a light yellow solid (1.24 g, 93%). The product was very hygroscopic, but could be stored in a desiccator over silica. FT-IR (ATR, cm<sup>-1</sup>): 3327 (NH<sub>2</sub>), 1656 (C=O). MS (MALDI-TOF, *m/z*): Calcd for C<sub>18</sub>H<sub>36</sub>N<sub>10</sub>O<sub>6</sub><sup>+</sup>: 488.28. Found: 488.36. <sup>1</sup>H NMR (DMSO-*d*<sub>6</sub>, δ/ppm): 7.62 (s, 6H), 7.14 (s, 6H), 3.04 (s, 12H), 2.53 (s, 12H). <sup>13</sup>C NMR (DMSO-*d*<sub>6</sub>, δ/ppm): 173.3, 59.1, 53.1, 52.5.

***N*-Benzyl-triethylenetetramine (8).** A mixture of benzaldehyde (48.8 cm<sup>3</sup>, 480 mmol) and triethylenetetramine (**7**) (78.0 g, 533 mmol) in EtOH–water (1 : 1, 425 cm<sup>3</sup>) was stirred for 15 minutes at RT. After cooling in an ice–water bath, sodium borohydride (12.1 g, 320 mmol) was added in small portions while maintaining the temperature below 15 °C. The mixture was stirred overnight at RT, then for 3 h at reflux temperature. After evaporation of the volatiles, water (300 cm<sup>3</sup>) was added and the suspension was extracted with *n*-butanol–toluene (1 : 1, 2 × 300 cm<sup>3</sup>). The solvents were removed by evaporation and the remains were fractionated with the aid of a Kugelrohr apparatus. Fractions containing more than 90% of **8** (as detected by NMR analysis) were combined and dissolved in EtOH. The solution was cooled in an ice–water bath and concentrated hydrochloric acid was added until no further precipitation occurred. A solid (22.4 g) was obtained after collection by filtration and drying. This raw product was used in the next step.

**Pentaethyl *N*-benzyl-triethylenetetramine-*N,N',N'',N''',N''''*-pentaacetate (9).** Triethylamine (36.2 cm<sup>3</sup>, 257 mmol) was added to a vigorously stirred suspension of the fine-mashed product of the previous reaction (**8**) (6.27 g) in toluene (250 cm<sup>3</sup>). Ethyl bromoacetate (25.5 cm<sup>3</sup>, 230 mmol) was added dropwise. After stirring for 6 d at RT and evaporation of the volatiles, chloroform (250 cm<sup>3</sup>) was added. The resulting solution was extracted with water (2 × 100 cm<sup>3</sup>), dried over magnesium sulfate, and the solvent of the organic phase was evaporated. The excess of ethyl bromoacetate was removed with the aid of a Kugelrohr apparatus. The product was obtained as a yellow oil (1.88 g, 2% overall yield over two reaction steps) after column chromatography (silica, solvent: ethyl acetate–heptane (4 : 1)). <sup>1</sup>H NMR (CDCl<sub>3</sub>, δ/ppm): 7.18 (m, 5H), 4.16 (q, *J* = 7.1 Hz, 6H), 4.14 (q, *J* = 7.1 Hz, 4H), 3.79 (s, 2H), 3.57 (s, 4H), 3.46 (s, 2H), 3.45 (s, 2H), 3.38 (s, 2H), 2.79 (t, *J* = 6.3 Hz, 2H), 2.76 (s, 4H), 2.69 (t, *J* = 6.3 Hz, 2H), 2.68 (s, 4H), 1.27 (t, *J* = 7.1 Hz, 15H).

***N*-Benzyl-triethylenetetramine-*N,N',N'',N''',N''''*-pentaacetamide (1btppam).** This compound was obtained as a white powder in 58% yield following the synthesis protocol of ttham, using **9** instead of **2**. FT-IR (ATR, cm<sup>-1</sup>): 3374 (NH<sub>2</sub>), 1688 and 1630 (C=O). MS (MALDI-TOF, *m/z*): Calcd for C<sub>23</sub>H<sub>39</sub>N<sub>9</sub>O<sub>5</sub><sup>+</sup>: 521.31. Found: 521.23. <sup>1</sup>H NMR (DMSO-*d*<sub>6</sub>, δ/ppm): 7.61 (s, 2H), 7.4–7.6 (broad, 5H), 7.25–7.15 (broad, 3H), 7.13 (s, 2H), 7.10 (s, 1H), 7.06 (s, 2H), 3.63 (s, 2H), 3.02 (s, 4H), 2.94 (s, 6H), 2.7–2.4 (broad, 12H). <sup>13</sup>C NMR (DMSO-*d*<sub>6</sub>, δ/ppm): 173.4, 173.2, 139.0, 129.3, 128.6, 127.4, 59.2, 58.9, 58.4, 57.5, 53.3, 53.2, 53.1, 52.4.

**tert-Butyl *N*-benzyl-ethylenediamine-*N'*-acetate (11).** A solution of *tert*-butyl 2-bromoacetate (1.64 cm<sup>3</sup>, 11.1 mmol) in DMF (15 cm<sup>3</sup>) was added dropwise over a period of 1.5 h to a stirred solution of *N*-benzylethylenediamine (5.00 g, 33.3 mmol) in DMF (100 cm<sup>3</sup>), which was cooled in an ice–water bath. Stirring was continued for 1 d. The reaction mixture was poured into water (200 cm<sup>3</sup>), followed by extraction with toluene (200 cm<sup>3</sup>). The organic layer was extracted with water (2 × 100 cm<sup>3</sup>), dried over magnesium sulfate, and the solvents were removed by evaporation to afford **11** as a viscous, light yellow liquid (2.8 g, 95%). <sup>1</sup>H NMR (CDCl<sub>3</sub>, δ/ppm): 7.18 (m, 5H), 3.79 (s, 2H), 3.24 (s, 2H), 2.75 (s, 4H), 1.72 (br., 2H), 1.44 (s, 9H).

**Penta-*tert*-butyl *N'*-benzyl-triethylenetetramine-*N,N,N',N''',N''''*-pentaacetate (13).** A solution of **11** (6.65 g, 25.2 mmol) in DMF (10 cm<sup>3</sup>) was added dropwise to a stirred mixture of di-*tert*-butyl 2-bromoethylamine-*N,N*-diacetate (**12**) (17.7 g, 50.3 mmol), sodium bicarbonate (16.9 g, 202 mmol), and DMF (250 cm<sup>3</sup>), which was cooled in an ice–water bath. The mixture was stirred for 1 h in the ice–water bath, then for 5 d at 50 °C. It was poured into water (500 cm<sup>3</sup>), followed by extraction with toluene (2 × 150 cm<sup>3</sup>). The combined organic layers were washed with water (2 × 100 cm<sup>3</sup>) and dried over magnesium sulfate. Column chromatography (silica, solvent: ethyl acetate–heptane (2 : 1)) afforded pure **13** as a yellow oil (3.79 g, 18%). <sup>1</sup>H NMR (CDCl<sub>3</sub>, δ/ppm): 7.18 (m, 5H), 3.65 (s, 2H), 3.41 (s, 4H), 3.40 (s, 4H), 3.25 (s, 2H), 2.6–2.9 (m, 12H), 1.44 (s, 45H).

***N'*-Benzyl-triethylenetetramine-*N,N,N',N''',N''''*-pentaacetic acid (14).** A mixture of **13** (20.8 g, 25.6 mmol), phosphoric acid (85%) (45 cm<sup>3</sup>, 0.66 mol), and toluene (250 cm<sup>3</sup>) was stirred at RT in a nitrogen atmosphere for 48 h, then the toluene was decanted. The residual oil was stirred successively with dichloromethane (100 cm<sup>3</sup>), ethyl acetate (100 cm<sup>3</sup>), and ethanol (100 cm<sup>3</sup>), and each of the solvents was separated thereafter from the solidifying residue. Drying of the obtained solid at 100 °C under high vacuum yielded pure **14** (14 g, 100%). <sup>1</sup>H NMR (D<sub>2</sub>O, δ/ppm): 7.20 (m, 5H), 4.31 (s, 2H), 3.90 (s, 4H), 3.51 (s, 4H), 3.37 (s, 2H), 3.2–3.4 (m, 8H), 3.02 (t, *J* = 6.0 Hz, 2H), 2.95 (t, *J* = 6.0 Hz, 2H).

**Pentaethyl *N'*-benzyl-triethylenetetramine-*N,N,N',N''',N''''*-pentaacetate (15).** This compound was obtained as a yellow oil in 61% yield following the synthesis protocol of **2**, using **14** instead of **1**. <sup>1</sup>H NMR (CDCl<sub>3</sub>, δ/ppm): 7.18 (m, 5H), 4.15 (q, *J* = 7.1 Hz, 8H), 4.13 (q, *J* = 7.1 Hz, 2H), 3.57 (s, 2H), 3.51 (s, 4H), 3.50 (s, 4H), 3.39 (s, 2H), 2.7–2.9 (m, 8H), 2.5–2.6 (m, 4H), 1.25 (t, *J* = 7.1 Hz, 15H).

***N'*-Benzyl-triethylenetetramine-*N,N,N',N''',N''''*-pentaacetamide (4bttpam).** This compound was obtained as a cream colored solid in 86% yield following the synthesis protocol of ttham, using **15** instead of **2**. FT-IR (ATR, cm<sup>-1</sup>): 3339 (NH<sub>2</sub>), 1680 and 1647 (C=O). MS (MALDI-TOF, *m/z*): Calcd for C<sub>23</sub>H<sub>39</sub>N<sub>9</sub>O<sub>5</sub><sup>+</sup>: 521.31. Found: 521.27. <sup>1</sup>H NMR (DMSO-*d*<sub>6</sub>, δ/ppm): 7.60 (s, 2H), 7.58 (s, 2H), 7.2–7.4 (broad, 5H), 7.25 (s, 1H), 7.12 (s, 4H), 7.07 (s, 1H), 3.55 (s, 2H), 3.00 (s, 8H), 2.92 (s, 2H), 2.7–2.4 (broad, 12H). <sup>13</sup>C NMR (DMSO-*d*<sub>6</sub>, δ/ppm): 173.5, 173.2, 139.5, 129.1, 128.5, 127.2, 59.1, 58.8, 58.6, 53.3, 53.1, 53.0, 52.1, 52.0.

**[Yb(ttham)]Cl<sub>3</sub>.** To a suspension of ttham (0.50 g, 1.0 mmol) in methanol (30 cm<sup>3</sup>) was added YbCl<sub>3</sub>·6H<sub>2</sub>O (0.39 g, 1.0 mmol). The

suspension was heated under reflux for 0.5 h, whereupon a clear solution was obtained (within a few minutes). At RT, propionitrile (50 cm<sup>3</sup>) was added and the solution was filtered into a covered crystallization dish. Overnight needle-like crystals were formed, which were collected by filtration, washed with acetone, and dried. The product was recrystallized from methanol–propionitrile (1 : 2, 60 cm<sup>3</sup>) to obtain a white, crystalline product, which was dried and stored over silica (0.60 g, 75%). Anal. (%) Calcd for C<sub>18</sub>H<sub>36</sub>N<sub>10</sub>O<sub>6</sub>YbCl<sub>3</sub>·2H<sub>2</sub>O: C, 26.89; H 5.01; N 17.42; Yb, 21.52; Cl, 13.23. Found: C, 27.00; H, 5.00; N, 17.10; Yb, 21.58; Cl, 12.53. FT-IR (ATR, cm<sup>-1</sup>): 3549 (w, br), 3250 (br), 3150 (br), 1676 (C=O), 1649 (C=O), 1604 (C=O), 1461, 1430, 1412, 1322, 1285, 1092, 920, 958, 896, 659, 429. MS (MALDI-TOF, *m/z*): Calcd for [Yb(ttham) – 2H]<sup>+</sup>: 660.21. Found: 660.17. MS (ESI, *m/z*): Calcd for [Yb(ttham) – 2H]<sup>+</sup>: 660.21. Found: 660.10.

**[Yb(1bttpam)]Cl<sub>3</sub>.** The compound was prepared following the synthesis protocol of [Yb(ttham)]Cl<sub>3</sub> starting from 1bttpam (0.31 g, 0.59 mmol) and YbCl<sub>3</sub>·6H<sub>2</sub>O (0.23 g, 0.59 mmol). The product was obtained as white crystals (0.49 g, 83%). Anal. (%) Calcd for C<sub>23</sub>H<sub>39</sub>N<sub>9</sub>O<sub>5</sub>YbCl<sub>3</sub>·3H<sub>2</sub>O: C, 32.31; H, 5.30; N, 14.74; Yb, 20.24; Cl, 12.44. Found: C, 32.50; H, 5.44; N, 14.10; Yb, 20.52; Cl, 12.29. FT-IR (ATR, cm<sup>-1</sup>): 3305 (br), 3123 (br), 1666 (C=O), 1599 (C=O), 1452, 1420, 1330, 1092, 917, 890, 652, 451, 431. MS (MALDI-TOF, *m/z*): Calcd for [Yb(1bttpam) – 2H]<sup>+</sup>: 693.23. Found: 693.09. MS (ESI, *m/z*): Calcd for [Yb(1bttpam) – 2H]<sup>+</sup>: 693.23. Found: 693.09.

**[Yb(4bttpam)]Cl<sub>3</sub>.** The compound was prepared following the synthesis protocol of [Yb(ttham)]Cl<sub>3</sub> starting from 4bttpam (0.50 g, 0.96 mmol) and YbCl<sub>3</sub>·6H<sub>2</sub>O (0.37 g, 0.96 mmol). The product was obtained as light yellow, needle-like crystals (0.65 g, 83%). Anal. (%) Calcd for C<sub>23</sub>H<sub>39</sub>N<sub>9</sub>O<sub>5</sub>YbCl<sub>3</sub>·3H<sub>2</sub>O: C, 32.31; H, 5.30; N, 14.74; Yb, 20.24; Cl, 12.44. Found: C, 32.30; H, 5.40; N, 14.30; Yb, 20.98; Cl, 11.98. FT-IR (ATR, cm<sup>-1</sup>): 3073 (br), 1660 (C=O), 1599 (C=O), 1453, 1430, 1323, 1119, 1098, 704, 648, 596, 457. MS (MALDI-TOF, *m/z*): Calcd for [Yb(4bttpam) – 2H]<sup>+</sup>: 693.23. Found: 693.16.

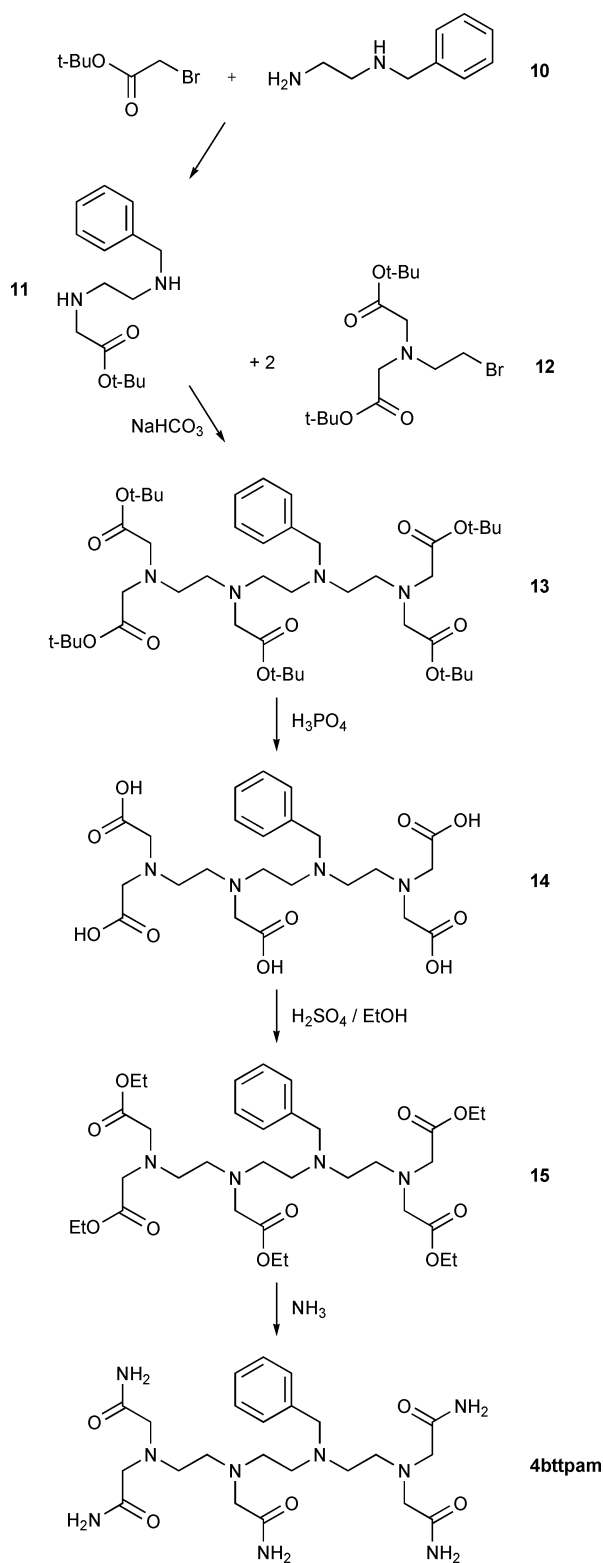
**Ytterbium chloride complexes of dtbam and ttham.** We were unsuccessful in crystallizing these very hygroscopic compounds. Samples of these complexes for NMR experiments were prepared *in situ* by stirring a buffered aqueous solution (20 mM MOPS, pH 7.40) containing the respective ligand (22 mM) and YbCl<sub>3</sub> (20 mM) at 80 °C for 2 h and subsequently at RT overnight. The pH was adjusted to 7.40. *Dtpam complex*: MS (HPLC-ESI): Calcd for [Yb(dtpam) – 2H]<sup>+</sup>: 560.14. Found: 560.14. *Tttham complex*: a large number of HPLC peaks was detected. The related MS spectra showed peaks at high *m/z* values, which are indicative of the formation of polymeric complexes in solution, but they could not be assigned unambiguously to particular multinuclear species.

## Results and discussion

### Synthesis

The ligands ttham, dtbam, and tttham were prepared by reaction of ammonia with their corresponding ethyl esters **2**, **4**, and **6**, respectively, in methanol following an earlier described procedure for the synthesis of *N,N,N',N'*-ethylenediaminetetraacetamide (Scheme 1).<sup>34</sup> The ethyl esters **2** and **4** were obtained in high





The mononuclear complexes  $[\text{Yb}(\text{L})]\text{Cl}_3$  ( $\text{L} = \text{ttham}, 1\text{btppam}, 4\text{btppam}$ ) were found to be highly water soluble and moderately hygroscopic as a solid. They could, nevertheless, be recrystallized from methanol–propionitrile. The crystallization of the ytterbium

complexes of the ligands dtpam and ttaham was however unsuccessful. From initially crystalline precipitates, only oily materials were obtained, which indicates that these materials are very hygroscopic. Samples of these metal complexes for NMR studies were therefore prepared *in situ* from stoichiometric amounts of the respective ligand and ytterbium trichloride in MOPS-buffered aqueous solution.

### Protonation constants

Table 1 summarizes the protonation constants (all in log values) determined for the five ligands of this study and compares these values with literature data for related acetamide- and methyl-substituted reference amines. The protonation constants are defined in eqn (3a) and (3b).



$$K_n = [\text{BH}_n^{n+}] / [\text{BH}_{(n-1)}^{(n-1)+}][\text{H}^+] \quad (3b)$$

With the exception of dtpam, all new ligands bear four tertiary amine groups. For each of those with a backbone derived from the linear triethylenetetramine (ttham, 1btppam, 4btppam) two protonation constants were determined, whereas only one protonation constant could be determined for the branched ttaham derivative as well as for the potentially tribasic dtpam ligand.

Based on the two protonation constants of the hexaacetamide ttham, which were determined to be 6.32 and 3.93, an equilibrium of three species is expected in the pH ranges between about 2 and 8. Fig. 1a shows the proton spectra of the ligand in  $\text{D}_2\text{O}$  solution in the pD range between 9.1 and 5.1. Above pD 8 (up to about pD 11, see supporting information, Fig. S1) four singlet peaks were observed with an intensity ratio of 8 : 4 : 8 : 4 (left to right). The two peaks at 3.30 and 3.21 ppm are assigned to methylene protons of the eight terminal (protons *a* in Scheme 4) and four central (*b*) acetamide groups, respectively. Likewise the second pair of resonances at 2.72 and 2.68 ppm is assigned to the two terminal (*c,d*) and one central (*e*) ethylene groups, respectively.

**Table 1** Protonation ( $\log K_i$ ) constants of acetamide- and methyl-substituted amine ligands (25 °C, 0.1 M  $\text{NaNO}_3$ )

Ligand <sup>a</sup>	$\log K_1$	$\log K_2$	$\log K_3$	$\log K_4$	Reference
ntam	2.6(1)	—	—	—	44
	2.47(2) <sup>b</sup>	—	—	—	51
edtam	4.36(2)	—	—	—	52
	4.57(1) <sup>b</sup>	—	—	—	51
dtpam	6.02(3)	—	—	—	This work
ttham	6.32(3)	3.93(3)	—	—	This work
1btppam	6.67(3)	5.08(3)	—	—	This work
4btppam	7.54(3)	4.01(3)	—	—	This work
ttaham	7.21(3)	—	—	—	This work
$\text{BzMe}_2\text{N}$	9.06	—	—	—	53
$\text{Me}_3\text{N}$	9.79(1)	—	—	—	54
	9.80	—	—	—	55
$\text{Me}_2\text{en}$	9.281(1)	6.130(2)	—	—	56
$\text{Me}_5\text{dien}$	9.42(1)	8.53(1)	2.08(1)	—	57
$\text{Me}_6\text{trien}$	9.11(2)	8.35(1)	5.26(3)	2.24(3)	58

<sup>a</sup>  $\text{BzMe}_2\text{N}$  = benzyldimethylamine;  $\text{Me}_3\text{N}$  = trimethylamine;  $\text{Me}_2\text{en}$  = *N,N,N',N'*-tetra(methyl)ethylenediamine;  $\text{Me}_5\text{dien}$  = *N,N,N',N'',N'''*-penta(methyl)diethylenetetramine;  $\text{Me}_6\text{trien}$  = *N,N,N',N'',N''',N''''*-hexa(methyl)triethylenepentamine. <sup>b</sup> 20 °C, 0.25 M KCl.

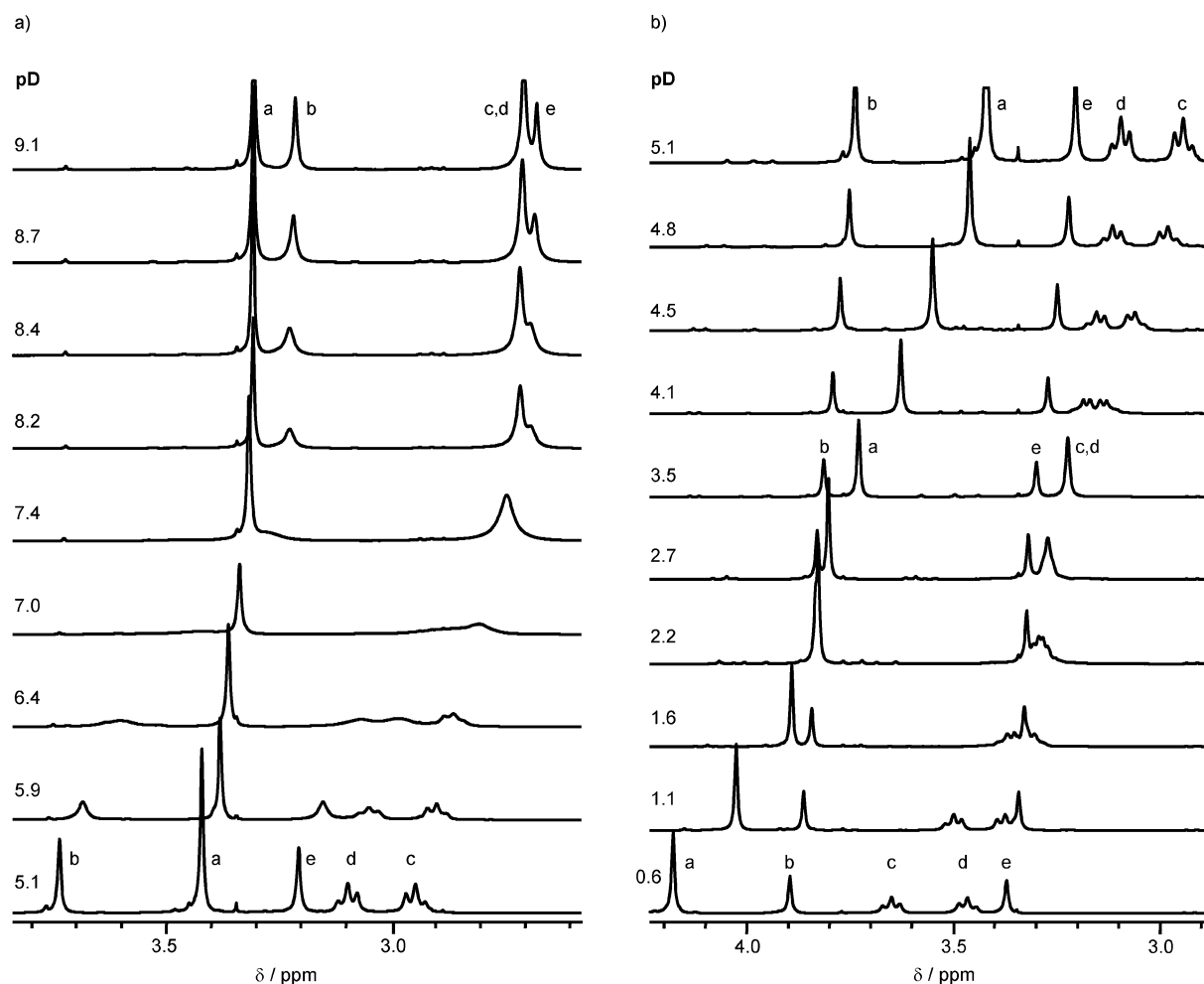
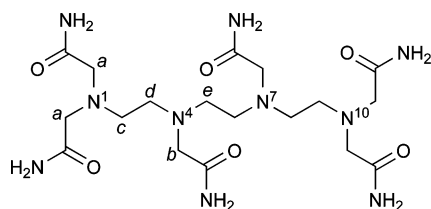


**Fig. 1**  $^1\text{H}$  NMR spectra of ttham solutions (30 mM) in  $\text{D}_2\text{O}$  at various pD values ( $\text{DNO}_3$ , KOD, no buffer,  $25^\circ\text{C}$ ). Chemical shifts ( $\delta$ ) are relative to the signal of sodium 3-(trimethylsilyl)-1-propanesulfonate (DSS,  $\delta = 0$  ppm) as the internal standard ( $c(\text{DSS}) = 3$  mM).



**Scheme 4**

In the first protonation step a strong change of the chemical shift of the central acetamide methylene groups (*b*) was observed, which increased from 3.30 to 3.74 ppm, whereas the resonance of the terminal methylene groups (*a*) was hardly affected. Protonation is known to cause deshielding of the protons that are close to the protonation sites, resulting in a downfield shift.<sup>35</sup> We therefore conclude that the first protonation is located predominantly at the central amine groups (N4 and N7). In accordance with this, upon protonation, the resonance of one ethylene group (assigned to the central ethylene group (*e*)) shifted significantly to 3.21 ppm and remained a singlet, whereas the remaining two groups now appeared as a set of two less shifted triplets. We assign these triplet peaks to the two terminal ethylene groups (*c,d*). On the NMR

timescale the monoprotinated ttham thus appears to show a two-fold symmetry. This suggests a fast equilibrium between mainly two tautomeric forms of  $\text{Httham}^+$  bearing the proton at either one of the two “central” amines, N4 or N7, while N1 and N10 remain unprotonated.<sup>36</sup> In other words, on the NMR time scale N4 and N7 share a single proton.

In the second protonation step of ttham the resonance of the four terminal acetamide methylene groups (*a*) became highly shifted from 3.42 ppm at pD 5.1 to about 3.75 ppm at pD 3.5 (Fig. 1b). Of the ethylene groups, now the central one (*e*) was hardly affected by the protonation, but the triplets of the two terminal groups (*c,d*) became shifted by some +0.2 ppm to reform a singlet, so that at pD 3.5 a spectrum comprising four singlet peaks was observed. It thus resembled the spectrum of the fully deprotonated ttham with the difference that now the peaks of the terminal methylene (*a*) and ethylene (*c,d*) groups had a smaller chemical shift than those of the respective central groups. The apparent symmetry of the doubly protonated ttham indicates that on the NMR timescale all four of the amino groups share equally a total of two protons, such that at any given time predominantly either N1 and N7, or N4 and N10 are each singly protonated. In fact, the second protonation constant of ttham is only slightly smaller ( $\Delta\log K = 0.5\text{--}0.6$ ) than the first protonation constant of

edtam (Table 1, Chart 3), which, considering the positive charge of the  $\text{H}^+\text{ttham}^+$ , is consistent with the assignment of the second protonation to occur at a terminal amine group.

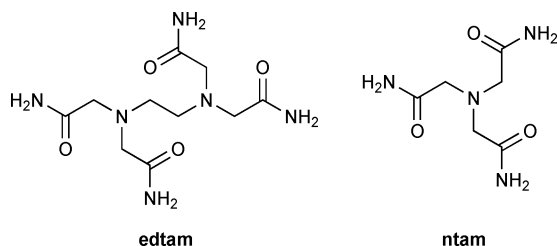


Chart 3

The spectra in Fig. 1b further suggest a third protonation of ttham below pD 2.7, which again is associated with a large shift of the aliphatic protons close to the terminal nitrogen atoms (*a,c,d*) accompanied by the reformation of a triplet signal of the terminal ethylene groups (*c,d*). It can therefore be concluded that the protonation of ttham follows the order N7, N1, N10, although the protonation constant of this third step has not been determined.

We did not attempt to quantify the fractions of protonation of the four backbone nitrogens.<sup>37</sup> Nevertheless, the above interpretation of the NMR data is consistent with NMR titration data reported for various terminal dtpa- and ttha-bis(amide) derivatives.<sup>38–41</sup> All of those are firstly protonated at the central backbone nitrogen, unless the amide nitrogens are bis(alkylated), which prevents the formation of a strong hydrogen bond system at the unprotonated terminal nitrogens. It was therefore not unexpected to find the first protonation constant of dtpam to be only 0.3 log *K* units smaller than that of ttham and not to be able to observe a second protonation step in the titration range of pH 1–8 (Table 1). The initial protonation at a central amine of both molecules makes the second protonation at a neighboring backbone nitrogen more difficult, which in the case of dtpam prevents a second protonation at a moderate pH, whereas in the case of ttham the second next nitrogen neighbor becomes protonated instead. Consequently the third proton is not placed between the first two protonation sites of ttham, but on the second terminal amine group to minimize the Coulomb repulsion between the positively charged ammonium groups.

The above protonation sequence of ttham is further supported by the protonation constants determined for its two benzyl derivatives 1btppam and 4btppam. The benzyl group itself is expected to cause a smaller decrease in basicity (compare  $\text{Me}_3\text{N}$  vs.  $\text{BzMe}_2\text{N}$  in Table 1) compared to the acetamide substituent. Therefore a relative increase in basicity upon substitution of an acetamide group with a benzyl group is indicative of a respective protonation site in the parent ttham ligand. In the case of 1btppam,

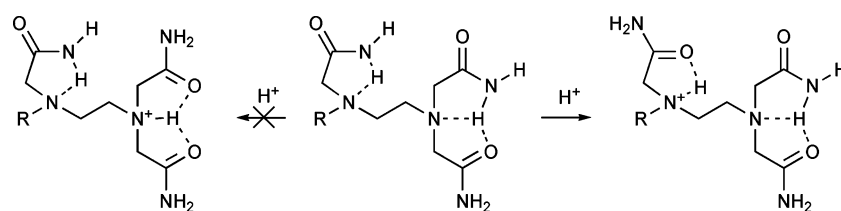
the first protonation step was much less affected by the substitution on N1 ( $\Delta\log K_1 \approx 0.35$ ) than the second proton addition ( $\Delta\log K_2 \approx 1.15$ ), which is consistent with a localization of this second protonation step on a terminal backbone nitrogen. The opposite was found for the N4 benzyl derivative 4btppam in comparison to ttham. The first protonation was facilitated ( $\Delta\log K_1 \approx 1.22$ ), whereas the addition of the second proton occurred at almost the same pH ( $\Delta\log K_2 < 0.1$ ). Both results are consistent with the proposed ttham protonation sequence of N7, N1, N10 (or N4, N10, N1, considering the symmetry of ttham).

In the case of dtpa-bis(amide)s, it had been shown that the unprotonated ligand is capable of forming two hydrogen bond ring systems that involve the amide hydrogens, the terminal nitrogens and the terminal carboxylate anion.<sup>39,42,43</sup> A very similar hydrogen bond network is expected to be formed at the terminal nitrogens of the per(amide)-substituted oligoamines, which involves both terminal acetamide groups (Scheme 5). The preference for the initial protonation of a central amino group can thus be explained considering that the addition of a proton to a terminal backbone nitrogen causes a destruction of this hydrogen bond system. A second consideration is the electron-withdrawing power of the acetamide substituent, which decreases the basicity of the amino group, making each acetamide-substituted ligand of Table 1 less strong a base compared to the respective permethylated ethylenamines.<sup>44</sup> This includes the ttham ligand, which does not bear an acetamide group directly linked to the central basic nitrogen. The direct and indirect impact of the acetamide substituent on the amine basicity are clearly illustrated by the decrease of log *K*<sub>1</sub> in the series ttham, dtpam, edtam, and ntam (Chart 3), in which zero, one, two, or three ( $\text{H}_2\text{NCOCH}_2$ )<sub>2</sub>NCH<sub>2</sub>CH<sub>2</sub> groups, respectively, of the basic amine are replaced with  $\text{H}_2\text{NCOCH}_2$  groups. Each substitution results in a decrease of log *K*<sub>1</sub> of about 1.2–2.0.

### NMR and CEST experiments

Water-suppressed <sup>1</sup>H NMR spectra of all ytterbium complexes were measured in aqueous buffer solution at pH 2.7 (red lines) and 7.4 (blue lines). Fig. 2 shows those of the ttham, 1btppam, and 4btppam complexes at 310 K. Since the exchange reaction of all amide protons with solvent water is fast under these conditions, their NMR resonances are very broad at pH 7.4.<sup>45</sup> They become detectable, however, at pH 2.7, where the base-catalyzed exchange reaction is sufficiently slow.

The ttham complex did not show any sharp resonances at pH 7.4 (Fig. 2a), but multiple broad resonances were observed between about –40 and +110 ppm. The spectrum at pH 2.7 revealed in addition two signals of exchangeable protons, which appeared as intensive, relatively sharp peaks at –14 and –27 ppm. They



Scheme 5

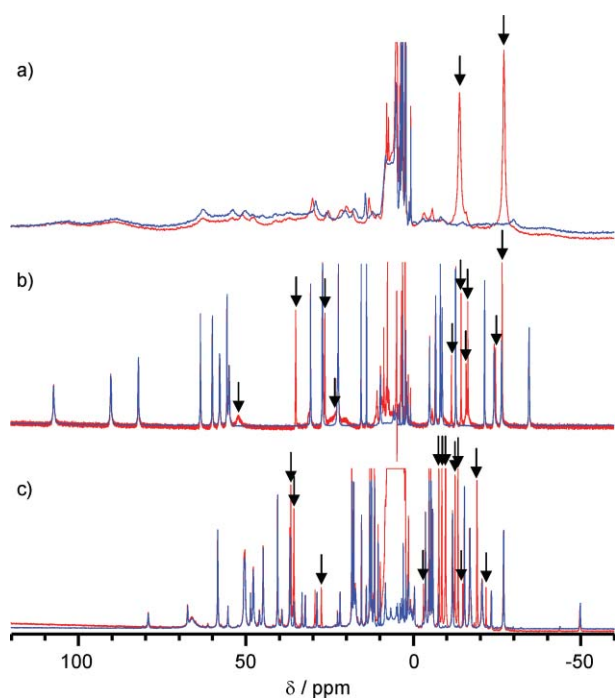


**Fig. 2**  $^1\text{H}$  NMR spectra of  $[\text{Yb}(\text{ttham})]^{3+}$  (a),  $[\text{Yb}(\text{1bttpam})]^{3+}$  (b), and  $[\text{Yb}(\text{4bttpam})]^{3+}$  (c) in aqueous solution ( $c(\text{complex}) = 20 \text{ mM}$ ,  $c(\text{MOPS}) = 10 \text{ mM}$ ,  $T = 310 \text{ K}$ ) at two pH values (7.40 (blue spectra), 2.70 (red spectra)). The water signal was suppressed by application of a continuous-wave presaturation pulse (1.5 s, 10  $\mu\text{T}$ ). Chemical shifts ( $\delta$ ) are relative to the resonance frequency of TMS ( $\delta = 0 \text{ ppm}$ ), approximated by setting the solvent water protons at 4.75 ppm. The resonances of exchangeable protons are indicated by arrows.

are assigned to the protons of ytterbium-bound amide groups. Unconstrained aminoacetamides coordinate to lanthanide ions *via* their oxygen atom such that the  $\text{NH}_2$  group points away from the metal ion. This results typically in a lower lanthanide induced shift of these protons compared to those of the backbone ethylene groups, which can show paramagnetic resonance shifts of some hundred ppm. The observed poorly resolved NMR resonances of the aliphatic protons are indicative of a flexible coordination geometry, possibly involving various structural isomers in an intermediate exchange regime. In such a situation the exchangeable resonances of the less chemically shifted amide protons can be in a fast exchange regime showing relatively sharp coalescence signals whereas the aliphatic protons remain in an intermediate exchange regime, which results in broad resonances.

Comparably well-defined were the resonances of the  $[\text{Yb}(\text{1bttpam})]\text{Cl}_3$  complex shown in Fig. 2b. At pH 7.4 the expected number of 29 C-H protons was matched by the observed number of sharp resonances between  $-40$  and  $+110 \text{ ppm}$ . From the spectrum at pH 2.7, after juxtaposition, the resonances of 10 exchangeable protons could be identified (indicated by arrows). The presence of individual resonances for all C-H protons is indicative of the absence of any apparent symmetry of this complex in solution, as expected based on the low symmetry of the 1bttpam ligand itself. The NMR spectrum is consistent with the coordination of all nine donor groups to the lanthanide ion. Directly comparing the 1bttpam and the ttham complexes, it appears that the substitution of the 1-benzyl group with a

sixth acetamide donor allows for the formation of coordination isomers in  $[\text{Yb}(\text{ttham})]^{3+}$ . Taking into account the broad NMR resonances, these isomers are considered to be in fast equilibrium exchange with each other. This situation is well known for the lanthanide complexes of the respective hexaacetic acid derivative  $\text{H}_6\text{ttha}$ .<sup>46,47</sup> In this case, on average only five of the six possible acetate donors are bound to the late lanthanide ions, resulting in a nonadentate coordination mode of the deprotonated  $\text{H}_6\text{ttha}$  ligand. Since one of the four terminal acetate groups remains uncoordinated, this opens the possibility of its quick exchange with any of the three coordinated and, based on the structure of the free ligand, symmetry-equivalent acetate groups.

To understand better, if  $[\text{Yb}(\text{ttham})]^{3+}$  behaves similarly, the NMR spectra of its 4bttpam derivative were recorded (Fig. 2c). In this case, one of the central acetamide ligands is substituted with a non-coordinating benzyl group, and a nonadentate coordination could only be achieved if, in addition to the four backbone amines and the central acetamide, all four terminal acetamides were involved. A large number of sharp NMR resonances were observed between  $-50$  and  $+80 \text{ ppm}$ . Judging from their number and their intensity distribution we suspect the presence of at least two conformational isomers in solution. Some 12 resonances of exchangeable protons could be identified, but we did not attempt an assignment of any of these peaks.

An overall comparison of the above NMR spectra, nevertheless, reveals a much higher similarity of the peak pattern found for  $[\text{Yb}(\text{ttham})]^{3+}$  (a) and  $[\text{Yb}(\text{1bttpam})]^{3+}$  (b) than for any other combination. Furthermore, in both of these spectra, peaks or clusters of peaks of exchangeable protons were found at about  $-14$  and  $-27 \text{ ppm}$ . We interpret this correspondence in terms of a high structural similarity of these two molecules, which in turn is in agreement with the above assumption that in the ttham complex on average one of the terminal acetamide donor groups remains uncoordinated. The appearance of only two amide peaks in the  $[\text{Yb}(\text{ttham})]^{3+}$  spectrum can be explained in terms of a spectral overlap of the six sharp individual amide peaks that were closely clustered around  $-14$  and  $-27 \text{ ppm}$  in the spectrum of the more rigid  $[\text{Yb}(\text{1bttpam})]^{3+}$ . Such a spectral overlap does not occur in case of the more isolated amide peaks that were observed between  $+20$  and  $+40 \text{ ppm}$  in the spectrum of the more rigid  $[\text{Yb}(\text{1bttpam})]^{3+}$ . The relatively high intensity of the negatively shifted amide peaks may be caused by a combination of this spectral overlap and the above discussed coalescence due to conformational exchange.

If this model is a good description of the situation in solution, a strong temperature dependence of the  $[\text{Yb}(\text{ttham})]^{3+}$  NMR spectrum is to be expected. NMR spectra of this complex between 293 and 353 K (Fig. 3) demonstrate the expected coalescence and subsequent sharpening of all resonances at higher temperatures, which is a good indication that all of them indeed stem from a set of isomers that exchange quickly with each other.

The differences in the NMR spectra of these three complexes are reflected in their CEST properties. A comparison of the respective Z spectra is shown in Fig. 4a. In these Z spectra the relative intensity of the bulk water signal is plotted as a function of the frequency offset of the applied presaturation RF pulse. Reference points are the resonance frequency of the solvent water on the frequency offset axis ( $\Delta\nu = 0 \text{ Hz}$ ) and the intensity of this signal, after

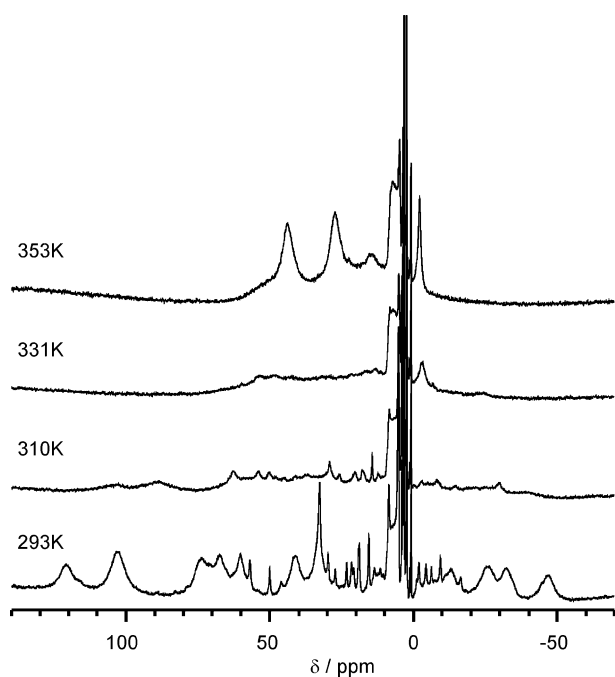


**Fig. 3**  $^1\text{H}$  NMR spectra of  $[\text{Yb}(\text{ttham})]^{3+}$  (20 mM) in aqueous solution ( $c(\text{MOPS}) = 10$  mM, pH 7.40) at four temperatures (293, 310, 331, and 353 K). The water signal was suppressed by application of a continuous-wave presaturation pulse (1.5 s, 10  $\mu\text{T}$ ). Chemical shifts ( $\delta$ ) are relative to the resonance frequency of TMS ( $\delta = 0$  ppm), approximated by setting the solvent water protons at 4.75 ppm.

a presaturation pulse with an “infinitely” large frequency offset ( $M_\infty$ ,  $\Delta\nu = \pm 200$  kHz) had been applied, on the intensity axis.

Both complexes,  $[\text{Yb}(\text{ttham})]^{3+}$  (black squares) and  $[\text{Yb}(\text{1bttpam})]^{3+}$  (red circles), exhibited peaks in their Z spectra that are indicative of saturation transfer at about  $-15$  and  $-30$  ppm, which is in good agreement with the above discussed exchangeable proton resonances found around  $-14$  and  $-27$  ppm. The Z-spectrum of  $[\text{Yb}(\text{1bttpam})]^{3+}$  further showed two relatively sharp signals between  $+20$  and  $+35$  ppm, which correspond nicely with at least two exchangeable-proton signals found in this region (Fig. 2b). This feature was also present in the  $[\text{Yb}(\text{ttham})]^{3+}$  Z spectrum (Fig. 4a), although no clear peak structure was resolved here. Taking into consideration that no sharp NMR resonances of exchangeable protons could be observed in this region (Fig. 2a), this suggests the presence of a dynamic process associated with these protons. These protons are apparently heavily affected by the fast conformational exchange reaction occurring in the dissolved  $[\text{Yb}(\text{ttham})]^{3+}$  complex. In support of the above discussed coordination model for the ttham complex, the Z spectrum of the  $[\text{Yb}(\text{4bttpam})]^{3+}$  complex (Fig. 4a) showed no clear similarities with that of  $[\text{Yb}(\text{ttham})]^{3+}$ .

For all three complexes, the realized CEST effect calculated according to eqn (1) is generally smaller than 50% at all frequencies. This is mainly a result of the appearance of CEST active proton resonances on both sides of the resonance of the bulk water signal. In this case, eqn (1) is not suitable to correct for the contribution of direct water saturation, which decreases symmetrically with increasing absolute offset frequency on both sides of this reference signal.

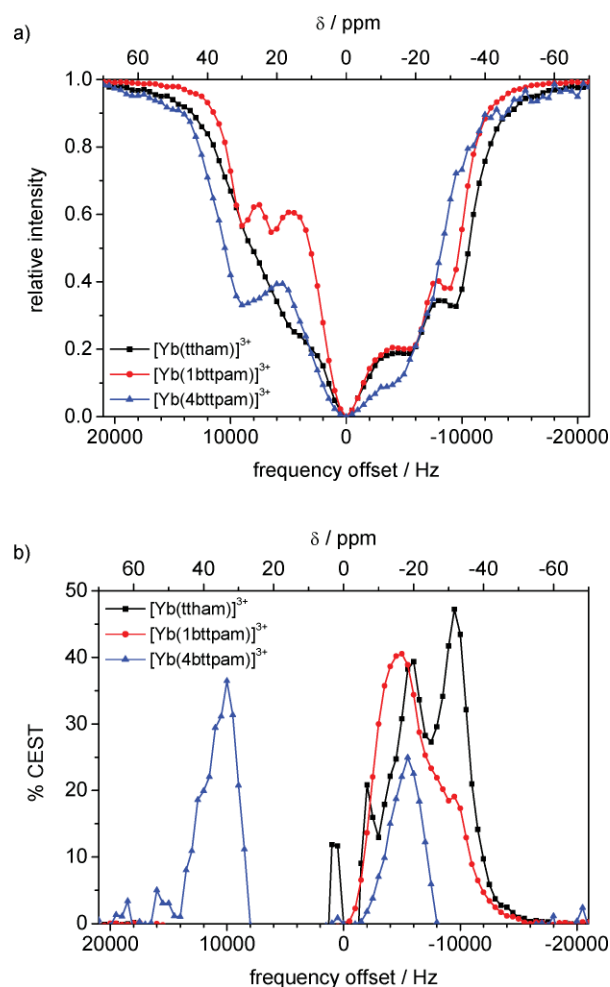


**Fig. 4** Proton Z spectra (a) and thereof calculated CEST spectra (b) of  $[\text{Yb}(\text{ttham})]^{3+}$ ,  $[\text{Yb}(\text{1bttpam})]^{3+}$ , and  $[\text{Yb}(\text{4bttpam})]^{3+}$  in aqueous solution ( $c(\text{complex}) = 20$  mM,  $c(\text{MOPS}) = 10$  mM,  $T = 310$  K, pH 7.40). Chemical shifts ( $\delta$ ) are relative to the resonance frequency of TMS ( $\delta = 0$  ppm), approximated by setting the solvent water protons at 4.75 ppm.

The  $^1\text{H}$  NMR spectra of the ytterbium complexes of the ttham and dtpam ligands both showed very broad peaks between  $-40$  and  $+40$  or  $+60$  ppm, respectively (Fig. 5). Both complexes exhibited exchangeable protons on both sides of the central bulk water resonance signal. These signals were sharp only in the case of the dtpam complex, which is indicative of a less dynamic solution structure. The absence of a clearly resolved pattern in the case of the ttham complex is consistent with observations made for the related hexaacetic acid derivative, which despite the three fold symmetry of the ligand itself, cannot coordinate with all six of its acetamide donor groups to a single lanthanide ion.<sup>48,49</sup> Hence, a situation similar to the above discussed  $[\text{Yb}(\text{ttham})]^{3+}$  case is likely, in which on average only two of the three equivalent  $(\text{H}_2\text{NCOCH}_2)_2\text{NCH}_2\text{CH}_2$  groups are coordinated to the ytterbium ion.

The Z spectra of the ttham and dtpam complexes depicted in Fig. 6a both showed only broad shoulders between  $-20$  and  $+20$  ppm, the chemical shift range, in which exchangeable protons were identified in the respective NMR spectra. The distribution of CEST-active resonances on both sides of the central water

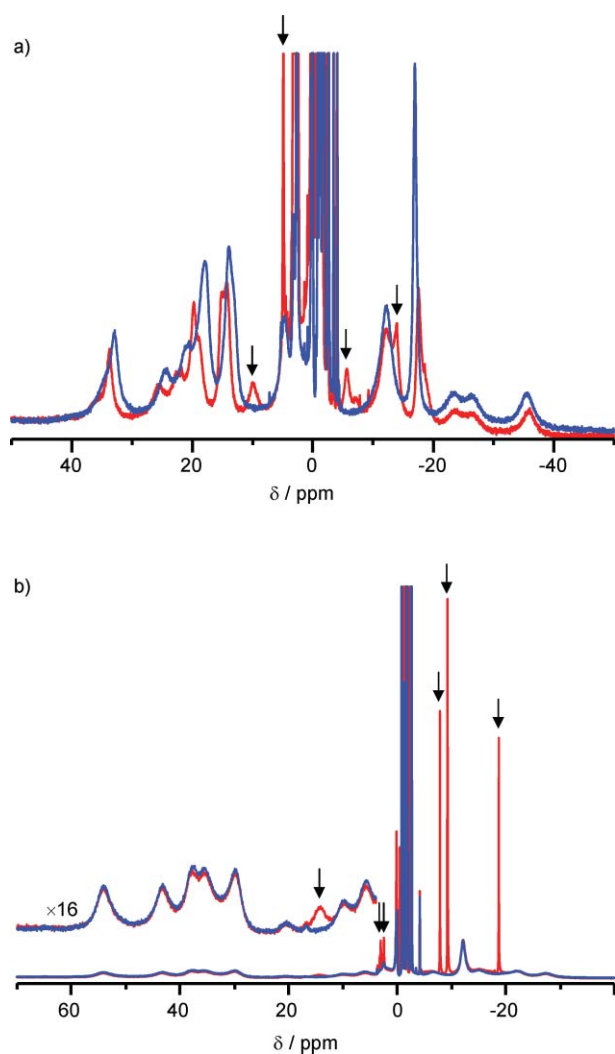


**Fig. 5**  $^1\text{H}$  NMR spectra of Yb complexes of ttaham (a) and dtpam (b) in aqueous solution ( $c(\text{YbCl}_3) = 20$  mM,  $c(\text{ligand}) = 22$  mM,  $c(\text{MOPS}) = 10$  mM,  $T = 310$  K) at two pH values (7.40 (blue spectra), 2.70 (red spectra)). The water signal was suppressed by application of a continuous-wave presaturation pulse (1.5 s, 10  $\mu\text{T}$ ).  $\delta$  Values are relative to the resonance frequency of TMS ( $\delta = 0$  ppm), approximated by setting the solvent water protons at 4.75 ppm. The resonances of exchangeable protons are indicated by arrows.

resonance results for both complexes in only small realized CEST effects based on eqn (1), not exceeding 35% at a metal concentration of 20 mM and at an optimized power level of the presaturation pulse (Fig. S2 and S3).

The discussed structural differences are reflected in the longitudinal water proton relaxivities  $r_1$  of the ytterbium complexes at 7 T as summarized in Table 2. The sterically constrained ttaham ligand is expected to allow for the coordination of one to two water molecules per ytterbium ion and as expected showed a relaxivity almost as high as the respective  $[\text{Yb}(\text{dota})(\text{H}_2\text{O})]^-$  complex.<sup>50</sup> The dotam and dtpam complexes showed a somewhat smaller relaxivity, which is consistent with the assumption that both bear not more than one water molecule in the first coordination sphere. As anticipated, the ytterbium complexes of the three trien-based acetamide ligands ttaham, 1btppam, 4btppam showed comparably small relaxivities in the order 4btppam > ttaham > 1btppam. This

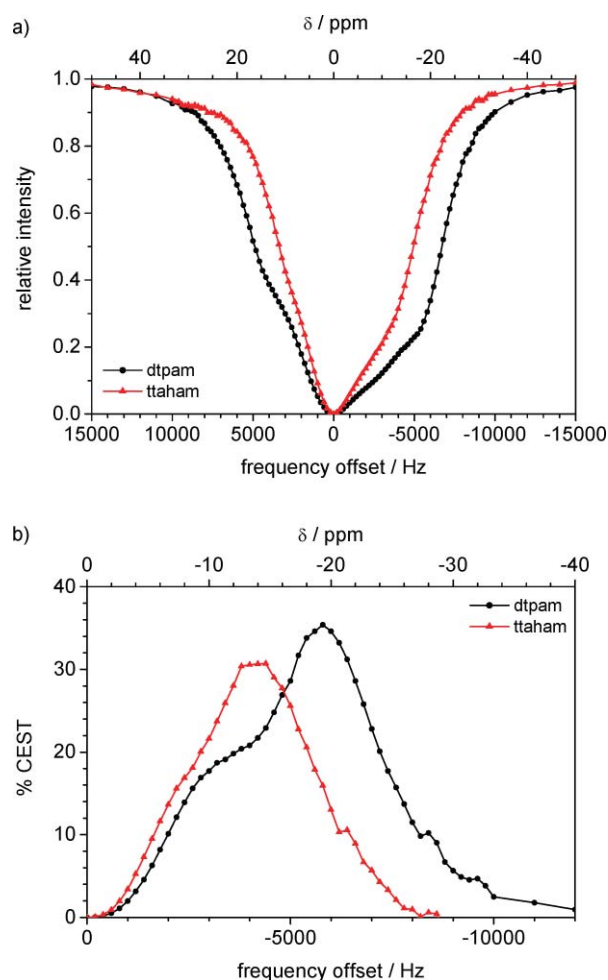


**Fig. 6** Proton Z spectra (a) and thereof calculated CEST spectra (b) of Yb complexes of dtpam and ttaham in aqueous solution ( $c(\text{YbCl}_3) = 20$  mM,  $c(\text{ligand}) = 22$  mM,  $c(\text{MOPS}) = 10$  mM,  $T = 310$  K, pH 7.40). Chemical shifts ( $\delta$ ) are relative to the resonance frequency of TMS ( $\delta = 0$  ppm), approximated by setting the solvent water protons at 4.75 ppm.

**Table 2** Proton relaxivities of Yb complexes in aqueous buffer solution ( $c(\text{MOPS}) = 10$  mM, pH 7.40, 310 K, 7 T)

Ligand <sup>a</sup>	$(T_1)_{\text{obs}}/\text{s}$	$r_1^b/10^{-3} \text{ mM}^{-1} \text{ s}^{-1}$
ttaham	2.71	6.92
1btppam	2.96	5.39
4btppam	2.61	7.61
dotam	2.43	9.05
H <sub>4</sub> dota	1.91	14.7
dtpam	2.29	10.3
ttaham	2.06	12.7

<sup>a</sup> dotam = 1,4,7,10-tetraazacyclododecane-1,4,7,10-tetraacetamide; H<sub>4</sub>dota = 1,4,7,10-tetraazacyclododecane-1,4,7,10-tetra(acetic acid).

<sup>b</sup> Calculated as  $r_1 = [(1/T_1)_{\text{obs}} - (1/T_1)_{\text{dia}}]/c(\text{Yb})$ ,  $c(\text{Yb}) = 20$  mM,  $(T_1)_{\text{dia}} = 4.34$  s.

order is in line with the interpretation of their NMR spectra, from which a complete saturation of the first coordination sphere with nine donor groups was deduced. The coordination mode is relatively rigid in the case of the 1btppam complex, which leaves no opening for a close interaction with water molecules. It is more

dynamic with respect to the terminal acetamide donors in the case of ttham, which may allow for a transiently closer interaction with the solvent water. Finally it involves an equilibrium with potentially significant structural changes in the case of the 4btppam complex, which would allow for an even more intense interaction of the ligand with water molecules. Overall the decrease in relaxivity of these coordinatively saturated complexes compared to  $[\text{Yb}(\text{dotam})(\text{H}_2\text{O})]^{3+}$  is nevertheless small. This clearly shows that the first coordination sphere contribution to the  $T_1$  relaxivity in these positively charged amide complexes is comparably small and second- and outer-sphere effects dominate.

## Conclusion

The five ligands ttham, 1btppam, 4btppam, ttaham, and dtppam were synthesized with the aim of forming lanthanide complexes suitable as contrast agents for magnetic resonance imaging applications utilizing the chemical exchange-dependent saturation transfer (CEST) effect. All ligands were characterized by their protonation constants and their complexation properties with ytterbium ions in aqueous solution.

In the case of the ttham ligand, three protonation steps of the backbone amino groups were characterized by  $^1\text{H}$  NMR spectroscopy. The basicity of these amino groups was found to decrease in the order  $N_{\text{central}(1)} > N_{\text{terminal}(1)} > N_{\text{terminal}(2)} > N_{\text{central}(2)}$ , as further deduced from a comparison of the protonation constants of ttham with those of the two ttham derivatives 1btppam and 4btppam, in which either a terminal or a central acetamide group is substituted with a benzyl group. The sequence of protonation is controlled by inductive effects of the substituents of the basic amine sites, the relative stability of the affected intramolecular hydrogen bonding networks, and the Coulomb repulsion between the different protonated ammonium groups.

The comparison between the  $^1\text{H}$  NMR properties of the ytterbium complexes of the ttham ligand and its two monobenzyl derivatives 1btppam and 4btppam led to the identification of a dynamic equilibrium in the ttham complex. The ytterbium complex of ttham is coordinatively frustrated, since due to steric constraints only three of the four symmetry-equivalent terminal acetamide donors can coordinate simultaneously to the ytterbium ion, and the dangling fourth one exchanges quickly with the other three. For all five studied ytterbium complexes, including those of the new ligands ttaham and dtppam, a number of exchangeable-proton resonances have been identified that were distributed over both positive and negative frequency offsets relative to the resonance peak of the bulk water signal. As a consequence of the low symmetry of these complexes, the thus high number of chemically different amide groups, and the presence of different coordination isomers that are in a fast equilibrium exchange with each other, the overall CEST effects were smaller than expected, when these ligands were designed to yield particularly high CEST effects in their ytterbium complexes bearing no lanthanide-coordinated water molecules. Our current studies are therefore directed towards a better understanding of the dynamics observed in these complexes and their influence on the complex stability with the aim of their further improvement for potential MR sensor applications. The results of these studies will be the subject of a subsequent publication.

## Acknowledgements

We thank our colleagues Danielle Beelen and Séverine Girard for NMR measurements, Piet Rommers for potentiometric measurements, Hugo Knobel for mass-spectrometric measurements, Thea Haex, Jeannette Smulders, Carry Hermans, and Adrie Jonkers for elemental analyses. We are grateful to our colleagues Holger Gröll, Sander Langereis, René Wegh, and Nico Willard for the fruitful collaboration and their very useful comments on the manuscript. Financial support by the Dutch government (Project code: BSIK 03033 “Molecular Imaging of Ischemic Heart Disease”) is gratefully acknowledged.

## References

- 1 S. Aime, M. Botta and E. Terreno, *Adv. Inorg. Chem.*, 2005, **57**, 173–237.
- 2 P. Caravan, J. J. Ellison, T. J. McMurry and R. B. Lauffer, *Chem. Rev.*, 1999, **99**, 2293–2352.
- 3 É. Tóth, L. Helm and A. E. Merbach, *Comprehensive Coordination Chemistry II*, Elsevier Pergamon, Amsterdam, 2004, vol. 9, pp. 841–881.
- 4 S. Aime, S. Geninatti Crich, E. Gianolio, G. B. Giovenzana, L. Tei and E. Terreno, *Coord. Chem. Rev.*, 2006, **250**, 1562–1579.
- 5 J. Zhou and P. C. M. van Zijl, *Prog. Nucl. Magn. Reson. Spectrosc.*, 2006, **48**, 109–136.
- 6 S. Aime, D. Delli Castelli and E. Terreno, *Angew. Chem., Int. Ed.*, 2005, **44**, 5513–5515.
- 7 S. Forsen and R. A. Hoffman, *J. Chem. Phys.*, 1963, **39**, 2892–2901.
- 8 S. Forsen and R. A. Hoffman, *J. Chem. Phys.*, 1964, **40**, 1189–1196.
- 9 M. Woods, D. E. Woessner and A. D. Sherry, *Chem. Soc. Rev.*, 2006, **35**, 500–511.
- 10 S. Zhang, M. Merritt, D. E. Woessner, R. E. Lenkinski and A. D. Sherry, *Acc. Chem. Res.*, 2003, **36**, 783–790.
- 11 K. M. Ward and R. S. Balaban, *Magn. Reson. Med.*, 2000, **44**, 799–802.
- 12 S. Aime, D. Delli Castelli and E. Terreno, *Angew. Chem., Int. Ed.*, 2002, **41**, 4334–4336.
- 13 J. A. Pikkemaat, R. T. Wegh, R. Lamerichs, R. A. van de Molengraaf, S. Langereis, D. Burdinski, A. Y. F. Raymond, H. M. Janssen, B. F. M. de Waal, N. P. Willard, E. W. Meijer and H. Gröll, *Contrast Media Mol. Imaging*, 2007, **2**, 229–239.
- 14 S. Zhang, C. R. Malloy and A. D. Sherry, *J. Am. Chem. Soc.*, 2005, **127**, 17572–17573.
- 15 S. Aime, D. Delli Castelli, F. Fedeli and E. Terreno, *J. Am. Chem. Soc.*, 2002, **124**, 9364–9365.
- 16 B. Yoo, M. S. Raam, R. M. Rosenblum and M. D. Pagel, *Contrast Media Mol. Imaging*, 2007, **2**, 189–198.
- 17 N. Goffeney, J. W. M. Bulte, J. Duyn, L. H. Bryant and P. C. M. van Zijl, *J. Am. Chem. Soc.*, 2001, **123**, 8628–8629.
- 18 S. Aime, D. Delli Castelli and E. Terreno, *Angew. Chem., Int. Ed.*, 2003, **42**, 4527–4529.
- 19 P. M. Winter, K. Cai, J. Chen, C. R. Adair, G. E. Kiefer, P. S. Athey, P. J. Gaffney, C. E. Buff, J. D. Robertson, S. D. Caruthers, S. A. Wickline and G. M. Lanza, *Magn. Reson. Med.*, 2006, **56**, 1384–1388.
- 20 S. Zhang, L. Michaudet, S. Burgess and A. D. Sherry, *Angew. Chem., Int. Ed.*, 2002, **41**, 1919–1921.
- 21 S. Aime, A. Barge, D. Delli Castelli, F. Fedeli, A. Mortillaro, F. U. Nielsen and E. Terreno, *Magn. Reson. Med.*, 2002, **47**, 639–648.
- 22 E. Terreno, D. Delli Castelli, G. Cravotto, L. Milone and S. Aime, *Invest. Radiol.*, 2004, **39**, 235–243.
- 23 D. Burdinski, J. Lub, J. A. Pikkemaat, H. Gröll, L. Nieto Garrido, S. G. Girard, D. Moreno Jalón and T. Weyhermüller, *JBIC, J. Biol. Inorg. Chem.*, 2007, **17**, S17–S17.
- 24 D. Burdinski, J. Lub, J. A. Pikkemaat, R. T. Wegh, H. Gröll, L. Nieto Garrido, S. G. Girard, S. Martial, C. Del Pozo Ochoa, D. Moreno Jalón and T. Weyhermüller, *Proc. Int. Soc. Magn. Reson. Med.*, 2007, **15**, 1182–1182.
- 25 R.-Y. Wang, J.-R. Lia, T.-Z. Jina, G.-X. Xua, Z.-Y. Zhou and X.-G. Zhou, *Polyhedron*, 1997, **16**, 2037–2040.
- 26 J. Wang, Z.-R. Liu, X.-D. Zhang, W.-G. Jia and H.-F. Li, *J. Mol. Struct.*, 2003, **644**, 29–36.

- 27 A. Mondry and P. Starynowicz, *New J. Chem.*, 2000, **24**, 603–607.
- 28 R. Ruloff, P. Prokop, J. Sieler, E. Hoyer and L. Beyer, *Z. Naturforsch., B: Chem. Sci.*, 1996, **51**, 963–968.
- 29 M. A. Williams and H. Rapoport, *J. Org. Chem.*, 1993, **58**, 1151–1158.
- 30 S. Amin, J. R. Morrow, C. H. Lake and M. R. Churchill, *Angew. Chem., Int. Ed. Engl.*, 1994, **33**, 773–775.
- 31 S. Aime, A. Barge, M. Botta, A. S. De Sousa and D. Parker, *Angew. Chem., Int. Ed.*, 1998, **37**, 2673–2675.
- 32 A. K. Covington, M. Paabo, R. A. Robinson and R. G. Bates, *Anal. Chem.*, 1968, **40**, 700–706.
- 33 R. Lumry, E. Smith and R. Glantz, *J. Am. Chem. Soc.*, 1951, **73**, 4330–4340.
- 34 A. Badinand, A. Boucherle and C. Charbonier, *Bull. Soc. Chim. Fr.*, 1960, 382–383.
- 35 J. L. Sudmeier and C. N. Reilley, *Anal. Chem.*, 1964, **36**, 1707–1712.
- 36 Y. Fujiwara and C. N. Reilley, *Anal. Chem.*, 1968, **40**, 890–894.
- 37 J. L. Sudmeier and C. N. Reilley, *Anal. Chem.*, 1964, **36**, 1698–1706.
- 38 C. F. G. C. Geraldès, R. Delgado, A. M. Urbano, J. Costa, F. Jasanada and F. Nepveu, *J. Chem. Soc., Dalton Trans.*, 1995, 327–335.
- 39 C. F. G. C. Geraldès, A. M. Urbano, M. C. Alpoim, A. D. Sherry, K.-T. Kuan, R. Rajagopalan, F. Maton and R. N. Muller, *Magn. Reson. Imaging*, 1995, **13**, 401–420.
- 40 L. Sarka, I. Bányai, E. Brücher, R. Király, J. Platzek, B. Radüchel and H. Schmitt-Willich, *J. Chem. Soc., Dalton Trans.*, 2000, 3699–3703.
- 41 Z. Jászberényi, É. Tóth, T. Kálai, R. Király, L. Burai, E. Brücher, A. E. Merbach and K. Hideg, *Dalton Trans.*, 2005, 694–701.
- 42 D. H. White, L. A. deLearie, T. J. Dunn, E. N. Rizkalla, H. Imura and G. R. Choppin, *Invest. Radiol.*, 1991, **26**, S229–S231.
- 43 H. Imura, G. R. Choppin, W. P. Cacheris, L. A. de Learie, T. J. Dunn and D. H. White, *Inorg. Chim. Acta*, 1997, **258**, 227–236.
- 44 L. A. Clapp, C. J. Siddons, D. G. VanDerveer, J. H. Reibenspies, S. B. Jones and R. D. Hancock, *Dalton Trans.*, 2006, 2001–2007.
- 45 G. P. Connelly, Y. Bai, M.-F. Jeng and S. W. Englander, *Proteins: Struct., Funct., Genet.*, 1993, **17**, 87–92.
- 46 E. Zitha-Bovens, R. N. Muller, S. Laurent, L. V. Elst, C. F. G. C. Geraldès, H. v. Bekkum and J. A. Peters, *Helv. Chim. Acta*, 2005, **88**, 618–632.
- 47 B. Achour, J. Costa, R. Delgado, E. Garrigues, C. F. G. C. Geraldès, N. Korber, F. Nepveu and M. I. Prata, *Inorg. Chem.*, 1998, **37**, 2729–2740.
- 48 R. Ruloff, K. Arnold, L. Beyer, F. Eitze, W. Gründer, M. Wagner and E. Hoyer, *Z. Anorg. Allg. Chem.*, 1995, **621**, 807–811.
- 49 R. Ruloff, T. Gelbrich, J. Sieler, E. Hoyer and L. Beyer, *Z. Naturforsch., B: Chem. Sci.*, 1997, **52**, 805–809.
- 50 R. Ruloff, R. N. Muller, D. Pubanz and A. E. Merbach, *Inorg. Chim. Acta*, 1998, **275–276**, 15–23.
- 51 L. Przyborowski, *Rocz. Chem.*, 1970, **44**, 1883–1894.
- 52 L. A. Clapp, C. J. Siddons, J. R. Whitehead, D. G. VanDerveer, R. D. Rogers, S. T. Griffin, S. B. Jones and R. D. Hancock, *Inorg. Chem.*, 2005, **44**, 8495–8502.
- 53 F. Wang and L. M. Sayre, *J. Am. Chem. Soc.*, 1992, **114**, 248–255.
- 54 P. Paoletti, J. H. Stern and A. Vacca, *J. Phys. Chem.*, 1965, **69**, 3759–3762.
- 55 E. Grunwald and E. K. Ralph, *Acc. Chem. Res.*, 1971, **4**, 107–113.
- 56 P. Paoletti, R. Barbucci, A. Vacca and A. Dei, *J. Chem. Soc. A*, 1971, 310–313.
- 57 D. Kroczevska, K. Bogusz, B. Kurzak and J. Jezierska, *Polyhedron*, 2002, **21**, 295–303.
- 58 R. Barbucci, V. Barone, M. Micheloni and L. Rusconi, *J. Phys. Chem.*, 1981, **85**, 64–68.